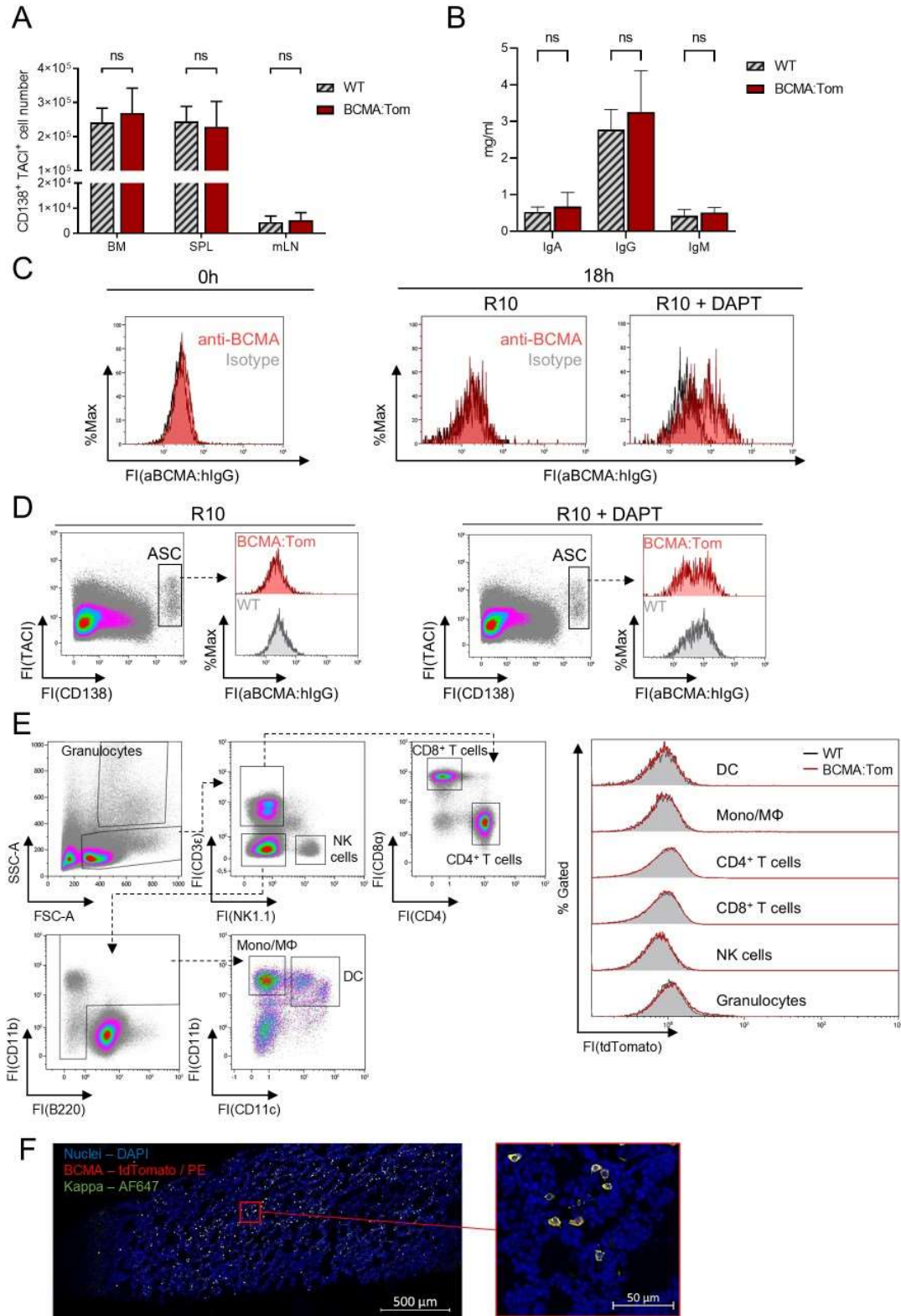


# **SUPPLEMENTAL MATERIAL**

**Schulz et al.**

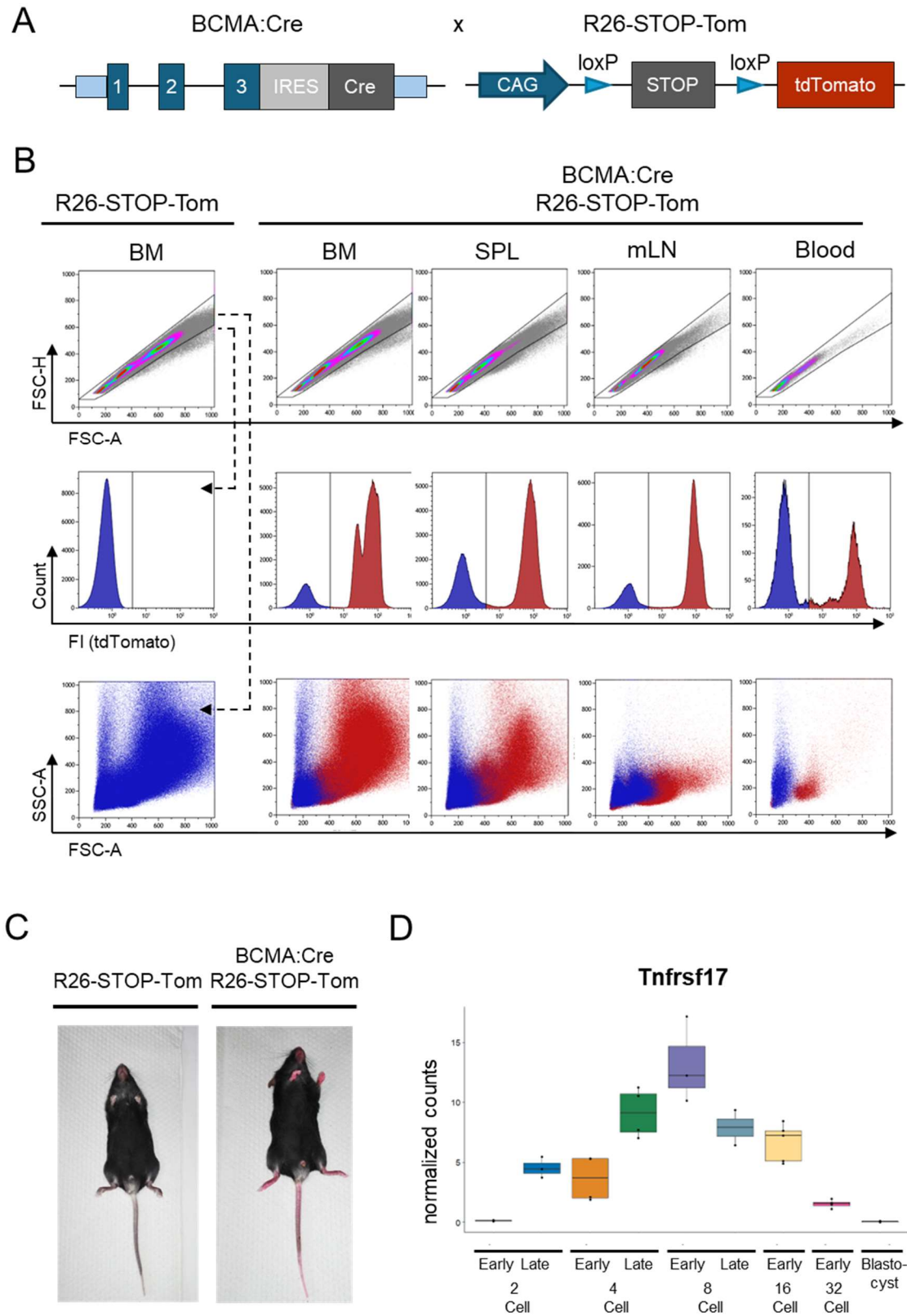
Decoding Plasma Cell Maturation Dynamics with BCMA

## ***Supplemental Figures***



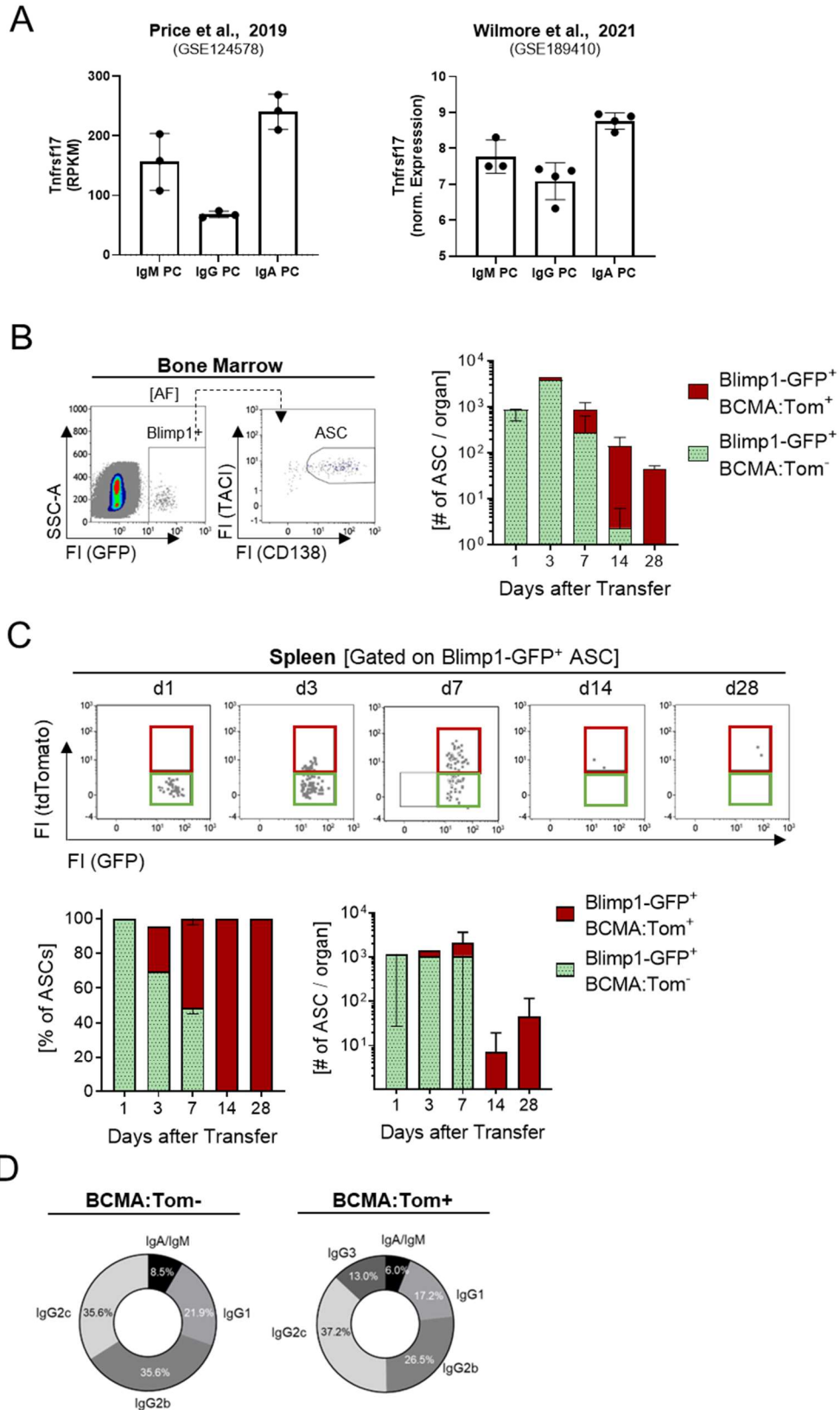
**Supplementary Figure 1. Characterization of BCMA:Tom mice.**

**Supplementary Figure 1. Characterization of BCMA:Tom mice.** (A) Absolute numbers of CD138<sup>+</sup> TACI<sup>+</sup> antibody-secreting cells (ASC) in the bone marrow (BM), spleen (SPL) and mesenteric lymph node (mLN) of unimmunized BCMA:Tom mice and wildtype littermate controls (n=7-9 mice per group). (B) Serum concentrations of IgA, IgG and IgM of unimmunized BCMA:Tom mice and wildtype littermate controls (n=7-9 mice per group). Statistical analysis was performed using repeated-measures 2-way ANOVA with adjusted p-values (Sidak correction) for multiple comparisons. ns, not significant p > 0.05. (C) Bone marrow of Blimp1-GFP reporter mice was isolated and stained with anti-BCMA (clone 25C2) or the isotype control antibody (clone TRES480) before (0h) and after culture for 18h at 37°C/5% CO<sub>2</sub> in R10 medium with the  $\gamma$ -secretase inhibitor DAPT (1  $\mu$ M) or R10 control medium. Overlaid histograms display fluorescence intensities secondary staining with anti-human IgG in the CD138<sup>+</sup>Blimp1-GFP<sup>+</sup> ASC gate. (D) Representative flow cytometric analysis of BCMA surface expression in splenic ASCs. Splenocytes of BCMA:Tom reporter mice and WT controls were isolated and surface stained with anti-BCMA (clone 25C2) after 18h at 37°C/5% CO<sub>2</sub> in R10 medium with 1  $\mu$ M DAPT or R10 control medium. Histograms display fluorescence intensities of anti-BCMA after secondary staining with anti-human IgG in the ASC gate. (E) Representative gating strategy to characterize tdTomato reporter activity in major splenic immune cell lineages with overlaid histograms of tdTomato fluorescence intensity in BCMA:Tom (red) and wildtype (black) littermates in the gates described in the upper panel. NK = natural killer cells; Mono/M $\Phi$  = monocytes/macrophages; DC = dendritic cells. (F) Immunofluorescence of BCMA:Tom bone marrow cryo-sections. Fixed femoral bone marrow was stained with anti-mouse Kappa-AF647 (green) and rabbit-anti-RFP with an anti-rabbit-IgG PE-labeled secondary antibody (red). DAPI (blue) was added as a nuclear staining. Overlap between Kappa and tdTomato/PE Signal is depicted in yellow.



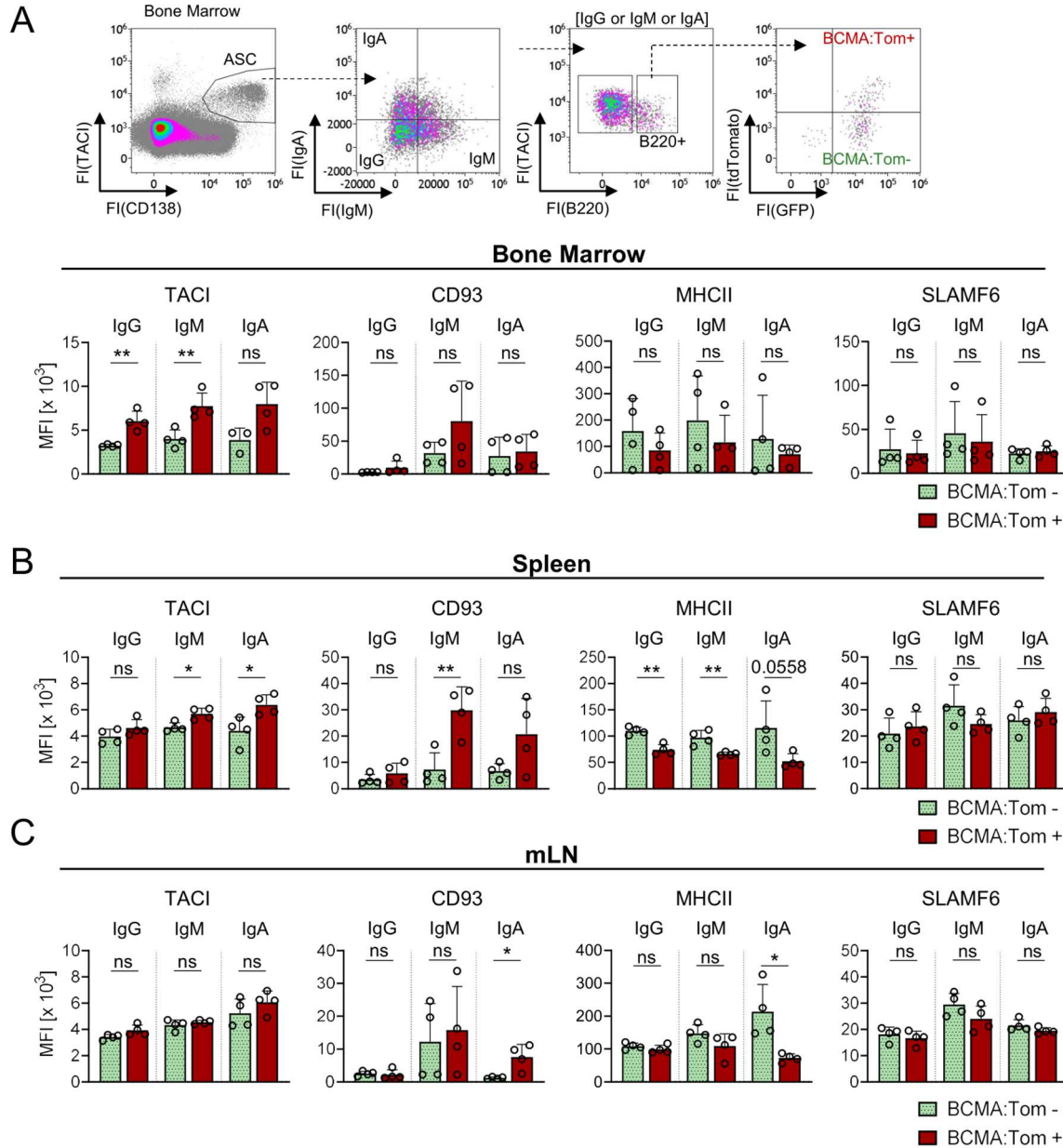
Supplementary Figure 2. BCMA:Cre deletes during early embryogenesis.

**Supplementary Figure 2. BCMA:Cre deletes during early embryogenesis.** (A) Schematic representation of the BCMA-Cre and R26-STOP-Tom (Ai9(RCL-tdT)) loci. (B) Flow cytometric analysis of bone marrow, spleen, mesenteric lymph nodes and blood of BCMA-Cre<sup>(+/-)</sup>/R26-STOP-Tomato mice or littermate R26-STOP-Tomato controls (representative results for n=3 animals). Singlets were gated based on FSC-H/FSC-A parameters and used as input for the tdTomato histogram and FSC/SSC dot-plot with tdTomato-positive events highlighted in red and -negative events colored in blue. (C) BCMA-Cre<sup>(+/-)</sup>/R26-STOP-Tomato mice show a bright red discoloration indicating deletion of the STOP-cassette in early progenitor cells. (D) Re-analysis of published RNA-Seq data of mouse pre-implantation embryos shows BCMA (*Tnfrsf17*) expression during early embryogenesis. The expression data was obtained from the GEO repository (GSE159484, Chi and Banerjee, 2020) and displayed as a boxplot of DESeq2-normalized counts).



**Supplementary Figure 3. BCMA expression and IgH isotype frequencies in plasma cell transcriptomes.**

**Supplementary Figure 3. BCMA expression and IgH isotype frequencies in plasma cell transcriptomes.** (A) Expression of BCMA (*Tnfrsf17*) in published transcriptomes of IgH isotype-sorted plasma cells from spleen (Price et al., 2019) and bone marrow (Wilmore et al., 2021). (B) Exemplary gating strategy to identify Blimp1-GFP-positive antibody-secreting cells (ASC) in the bone marrow of recipient mice after transfer and quantification of absolute cell numbers of Blimp1-GFP<sup>+</sup>BCMA:Tom<sup>-</sup> (green) and Blimp1-GFP<sup>+</sup>BCMA:Tom<sup>+</sup> (red) cells in bone marrow isolated from 2 femur and 2 tibiae of the recipient mice (mean  $\pm$  SD). Data shows n=3 mice/timepoint (except day 3 with one mouse analyzed). (C) Blimp1-GFP<sup>+</sup>CD138<sup>+</sup>TACI<sup>+</sup> ASCs in the spleen were quantified by flow cytometry at the indicated time points after transfer. The frequency and absolute number of Blimp1-GFP<sup>+</sup>BCMA:Tom<sup>-</sup> (green) and Blimp1GFP<sup>+</sup>BCMA:Tom<sup>+</sup> (red) cells at each timepoint are depicted (mean  $\pm$  SD). Data shows n=3 mice/timepoint (except day 3 with one mouse analyzed) (D) Mean frequencies of IgH-constant regions among clones extracted by MiXCR from BCMA:Tom<sup>-</sup> and BCMA:Tom<sup>+</sup> IgG plasma cell transcriptomes (n=4 per group).



**Supplementary Figure 4. BCMA expression correlates with surface marker abundance across B220<sup>+</sup> ASC isotypes and tissues.** (A) Selected markers were analyzed by flow cytometry on BCMA:Tom<sup>-</sup> (green) and BCMA:Tom<sup>+</sup> (red) B220<sup>+</sup> ASC in the bone marrow of unimmunized Blimp1-GFP/BCMA:Tom mice. The surface abundance of selected markers was analyzed for IgG-, IgM- or IgA-positive ASCs in the bone marrow. (B), (C) The protein abundance of selected markers of BCMA:Tom<sup>-</sup> and BCMA:Tom<sup>+</sup> ASC for the Ig heavy chain isotypes IgG, IgM and IgA are summarized in (B) spleen and (C) mLN. Median fluorescence intensities (MFI) are summarized in bar charts (mean  $\pm$  SD. Statistical analysis was performed using repeated-measures 2-way ANOVA with adjusted p-values (Sidak correction) for multiple comparisons (n=4 per group). ns = not significant, p > 0.05; \*, p < 0.05; \*\*, p < 0.01; \*\*\*, p < 0.001; \*\*\*\*, p < 0.0001.